Estimation of elastic stiffness parameters in weakly anisotropic rotated HTI media

David Cho (dwhcho@ucalgary.ca), Gary F. Margrave

ABSTRACT

The presence of fractures and directional in-situ stress fields in the subsurface has profound implications for numerous geophysical and engineering applications. These phenomenon manifest as azimuthal variations in the seismic response and can be detected in the amplitudes of the scattered wavefield. Therefore, the study of the azimuthal amplitude variation with offset (AVO) can provide information regarding the fracturing or the stress state of the subsurface.

In this study, a transversely isotropic medium with a horizontal axis of symmetry (HTI) was used to model the presence of fractures and directional in-situ stress fields. Previous formulations of the reflections from HTI media invoke conditions that are often unrealistic in the natural world. Therefore, a more generic HTI reflection model was presented. This involves a transformation of the elastic stiffness matrix to represent an unknown symmetry axis azimuth where it is allowed to vary as a function of depth. In addition, we investigate the effect of dipping fracture sets and when the vertical stress is not equal to one of the principle stresses. It is shown that the corresponding reflection coefficients for a transformed HTI medium is capable of resolving the symmetry axis azimuth but lacks the complete set of parameters required to characterize the dipping fractures or when the vertical stress is not equal to one of the principle stresses. However, a different parameterization of the model space in the parameter estimation problem can provide an inference as to the presence of dipping fractures or a non-vertical principle stress component. These concepts are illustrated through a numerical example.

INTRODUCTION

- Azimuthal anisotropy
  - Oriented fracture sets
    - Permeability pathways in subsurface formations
  - Directional in-situ stress fields
    - Fracture response in hydraulic stimulation
- Analysis of stress and strain relationship yields the elastic stiffness parameters that characterize medium
- Reflection seismic experiment
  - Stresses imposed by incident wavefield results in strains that can be detected by scattered wavefield
  - Analysis of reflection coefficients (azimuthal AVO) provides the means to estimate elastic stiffness coefficients
    - Infer presence of fractures and determine in-situ stress field
- HTI medium
  - Model to represent vertical aligned fractures or directional horizontal stresses
  - Previous HTI reflection models represent unrealistic scenarios
  - Present a more generic HTI reflection model
    - Discuss implications for the parameter estimation problem

HTI MEDIA UNDER A COORDINATE ROTATION

- Rotate an HTI medium in its natural coordinate system about the x_2 and x_3 axes
  - Rotation about x_2 axis – Dipping fractures or non-vertical principle stress
  - Rotation about x_{23} axis – Unknown symmetry axis azimuth
  - Bond transformation
    - $\underline{\underline{A}} = \underline{\underline{M}}\,\underline{\underline{A^n}}\,\underline{\underline{M}}^T$

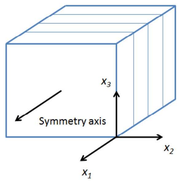

FIG. 1. HTI media in its natural coordinate system where the symmetry axis coincides with the x_1 axis.

$$\underline{\underline{A^n}} = \begin{bmatrix} A^n_{11} & A^n_{12} & A^n_{13} & 0 & 0 & 0 \\ A^n_{12} & A^n_{22} & A^n_{23} & 0 & 0 & 0 \\ A^n_{13} & A^n_{23} & A^n_{33} & 0 & 0 & 0 \\ 0 & 0 & 0 & A^n_{44} & 0 & 0 \\ 0 & 0 & 0 & 0 & A^n_{55} & 0 \\ 0 & 0 & 0 & 0 & 0 & A^n_{66} \end{bmatrix}$$

$$A^n_{33} = A^n_{22}, A^n_{55} = A^n_{66},\ A^n_{13} = A^n_{12}, A^n_{23} = A^n_{33} - 2A^n_{44}$$

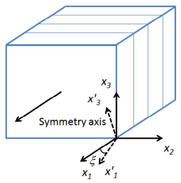

FIG. 2. HTI media under a coordinate rotation about the x_2 axis by an angle ξ.

$$\underline{\underline{M(\xi)}} = \begin{bmatrix} \cos^2\xi & 0 & \sin^2\xi & 0 & -\sin 2\xi & 0 \\ 0 & 1 & 0 & 0 & 0 & 0 \\ \sin^2\xi & 0 & \cos^2\xi & 0 & \sin 2\xi & 0 \\ 0 & 0 & 0 & \cos\xi & 0 & \sin\xi \\ \frac{\sin 2\xi}{2} & 0 & -\frac{\sin 2\xi}{2} & 0 & \cos 2\xi & 0 \\ 0 & 0 & 0 & -\sin\xi & 0 & \cos\xi \end{bmatrix}$$

$$\underline{\underline{A(\xi)}} = \begin{bmatrix} A_{11}(\xi) & A_{12}(\xi) & A_{13}(\xi) & 0 & A_{15}(\xi) & 0 \\ A_{12}(\xi) & A_{22}(\xi) & A_{23}(\xi) & 0 & A_{25}(\xi) & 0 \\ A_{13}(\xi) & A_{23}(\xi) & A_{33}(\xi) & 0 & A_{35}(\xi) & 0 \\ 0 & 0 & 0 & A_{44}(\xi) & 0 & A_{46}(\xi) \\ A_{15}(\xi) & A_{25}(\xi) & A_{35}(\xi) & 0 & A_{55}(\xi) & 0 \\ 0 & 0 & 0 & A_{46}(\xi) & 0 & A_{66}(\xi) \end{bmatrix}$$

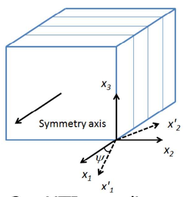

FIG. 3. HTI media under a coordinate rotation about the x_3 axis by an angle ψ.

$$\underline{\underline{M(\psi)}} = \begin{bmatrix} \cos^2\psi & \sin^2\psi & 0 & 0 & 0 & \sin 2\psi \\ \sin^2\psi & \cos^2\psi & 0 & 0 & 0 & -\sin 2\psi \\ 0 & 0 & 1 & 0 & 0 & 0 \\ 0 & 0 & 0 & \cos\psi & -\sin\psi & 0 \\ 0 & 0 & 0 & \sin\psi & \cos\psi & 0 \\ -\frac{\sin 2\psi}{2} & \frac{\sin 2\psi}{2} & 0 & 0 & 0 & \cos 2\psi \end{bmatrix}$$

$$\underline{\underline{A(\psi)}} = \begin{bmatrix} A_{11}(\psi) & A_{12}(\psi) & A_{13}(\psi) & 0 & 0 & A_{16}(\psi) \\ A_{12}(\psi) & A_{22}(\psi) & A_{23}(\psi) & 0 & 0 & A_{26}(\psi) \\ A_{13}(\psi) & A_{23}(\psi) & A_{33}(\psi) & 0 & 0 & A_{36}(\psi) \\ 0 & 0 & 0 & A_{44}(\psi) & A_{45}(\psi) & 0 \\ 0 & 0 & 0 & A_{45}(\psi) & A_{55}(\psi) & 0 \\ A_{16}(\psi) & A_{26}(\psi) & A_{36}(\psi) & 0 & 0 & A_{66}(\psi) \end{bmatrix}$$

RELECTION COEFFICIENTS FOR WEAKLY ANISOTRPIC HTI MEDIA

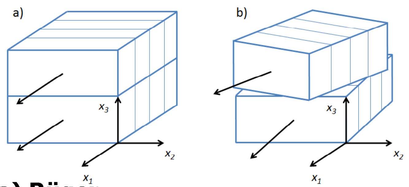

FIG. 4. HTI/HTI interface with a) similar symmetry axis orientations and b) arbitrary symmetry axis orientations.

a) Rüger

$$R_{pp}(\theta,\phi) = \frac{1}{2}\frac{\Delta Z}{\overline{Z}} + \frac{1}{2}\left[\frac{\Delta\alpha}{\overline{\alpha}} - \left(\frac{2\overline{\beta}}{\overline{\alpha}}\right)^2\frac{\Delta G}{\overline{G}}\right] + \left[\Delta\left(\frac{(A^n_{13}+A^n_{55})^2 - (A^n_{33}+A^n_{55})^2}{2A^n_{33}(A^n_{33}+A^n_{55})}\right) + 2\left(\frac{2\overline{\beta}}{\overline{\alpha}}\right)^2\Delta\left(\frac{(A^n_{44}-A^n_{66})}{2A^n_{66}}\right)\right]\cos^2\phi\sin^2\theta + \frac{1}{2}\left[\frac{\Delta\alpha}{\overline{\alpha}} + \Delta\left(\frac{(A^n_{11}-A^n_{33})}{2A^n_{33}}\right)\cos^4\phi + \Delta\left(\frac{(A^n_{13}+A^n_{55})^2 - (A^n_{33}+A^n_{55})^2}{2A^n_{33}(A^n_{33}+A^n_{55})}\right)\sin^2\phi\cos^2\phi\right]\sin^2\theta\tan^2\theta$$

$$B(\phi_k) = B^{iso} + B^{ani}\cos^2(\phi_k - \phi_{sym})$$

b) Vavryčuk and Pšenčík

$$R_{pp}(\theta,\phi) = R^{iso}_{pp}(\theta) + \frac{1}{2}\left[\Delta\left(\frac{A_{23}+2A_{44}-A_{33}}{A_{33}}\right)\sin^2\phi + \left(\Delta\left(\frac{A_{13}+2A_{55}-A_{33}}{A_{33}}\right) - 8\Delta\left(\frac{A_{55}-A_{44}}{2A_{33}}\right)\right)\cos^2\phi + 2\left[\Delta\left(\frac{A_{36}-A_{45}}{A_{33}}\right) - 4\Delta\left(\frac{A_{45}}{A_{33}}\right)\right]\cos\phi\sin\phi\right]\sin^2\theta + \frac{1}{2}\left[\Delta\left(\frac{A_{11}-A_{33}}{2A_{33}}\right)\cos^4\phi + \Delta\left(\frac{A_{22}-A_{33}}{2A_{33}}\right)\sin^4\phi + \Delta\left(\frac{A_{12}+2A_{66}-A_{33}}{A_{33}}\right)\cos^2\phi\sin^2\phi + 2\Delta\left(\frac{A_{16}}{A_{33}}\right)\cos^3\phi\sin\phi + 2\Delta\left(\frac{A_{26}}{A_{33}}\right)\sin^3\phi\cos\phi\right]\sin^2\theta\tan^2\theta$$

$$R^{iso}_{PP}(\theta) = \frac{1}{2}\frac{\Delta Z}{\overline{Z}} + \frac{1}{2}\left[\frac{\Delta\alpha}{\overline{\alpha}} - \left(\frac{2\overline{\beta}}{\overline{\alpha}}\right)^2\frac{\Delta G}{\overline{G}}\right]\sin^2\theta + \frac{1}{2}\frac{\Delta\alpha}{\overline{\alpha}}\sin^2\theta\tan^2\theta$$

THE PARAMETER ESTIMATION PROBLEM

- Downton and Roure (2010)
  - Estimation of fracture parameters using a simulated annealing technique
    - Parameterization of model space in terms of layer time thickness, P and S wave impedances, density, the Thomsen parameters delta, epsilon and gamma and the azimuth of the symmetry axis
- Vavryčuk and Pšenčík equation can be used to perform forward modeling
  - Elastic stiffness parameters are the same as rotated HTI medium about x_3
    - Symmetry axis azimuth can be recovered
  - Not all elastic stiffness parameters for rotation about x_2 are present
    - Dipping fractures or non-vertical principle stress can not be fully characterized
  - A_{12} and A_{66} are non-unique

NUMBERICAL EXAMPLE

$$\underline{\underline{A^n}} = \begin{bmatrix} 11.96 & 3.99 & 3.99 & 0 & 0 & 0 \\ 3.99 & 15.55 & 4.89 & 0 & 0 & 0 \\ 3.99 & 4.89 & 15.55 & 0 & 0 & 0 \\ 0 & 0 & 0 & 5.33 & 0 & 0 \\ 0 & 0 & 0 & 0 & 4.76 & 0 \\ 0 & 0 & 0 & 0 & 0 & 4.76 \end{bmatrix} \quad \underline{\underline{A(\xi=10)}} = \begin{bmatrix} 12.05 & 4.02 & 4.00 & 0 & -0.27 & 0 \\ 4.02 & 15.55 & 4.86 & 0 & -0.15 & 0 \\ 4.00 & 4.86 & 15.43 & 0 & -0.35 & 0 \\ 0 & 0 & 0 & 5.31 & 0 & -0.10 \\ -0.27 & -0.15 & -0.35 & 0 & 4.77 & 0 \\ 0 & 0 & 0 & -0.10 & 0 & 4.78 \end{bmatrix}$$

$$\underline{\underline{A(\xi=10,\psi=30)}} = \begin{bmatrix} 12.84 & 4.10 & 4.22 & 0.05 & -0.25 & 0.71 \\ 4.10 & 14.59 & 4.65 & 0.16 & -0.12 & 0.81 \\ 4.22 & 4.65 & 15.43 & 0.17 & -0.30 & 0.37 \\ 0.05 & 0.16 & 0.17 & 5.18 & 0.23 & -0.07 \\ -0.25 & -0.12 & -0.30 & 0.23 & 4.91 & 0.02 \\ 0.71 & 0.81 & 0.37 & -0.07 & 0.02 & 4.86 \end{bmatrix} \quad \underline{\underline{A^T(\xi,\psi)}} = \begin{bmatrix} 12.84 & 4.10 & 4.22 & 0 & 0 & 0.71 \\ 4.10 & 14.59 & 4.65 & 0 & 0 & 0.81 \\ 4.22 & 4.65 & 15.43 & 0 & 0 & 0.37 \\ 0 & 0 & 0 & 5.18 & 0.23 & 0 \\ 0 & 0 & 0 & 0.23 & 4.91 & 0 \\ 0.71 & 0.81 & 0.37 & 0 & 0 & 4.86 \end{bmatrix}$$

Condition for natural coordinate system $\max[A^n_{44} - A^n_{55}]$

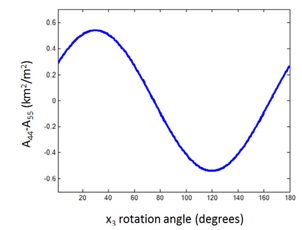

FIG. 5. Plot of A_{44}-A_{55} from zero to 180 degrees. The function reaches a maximum at 30 degrees, denoting the symmetry axis orientation.

$$\underline{\underline{A^{ne}}} = \begin{bmatrix} 12.05 & 4.02 & 4.00 & 0 & 0 & 0 \\ 4.02 & 15.55 & 4.86 & 0 & 0 & 0 \\ 4.00 & 4.86 & 15.43 & 0 & 0 & 0 \\ 0 & 0 & 0 & 5.31 & 0 & 0 \\ 0 & 0 & 0 & 0 & 4.77 & 0 \\ 0 & 0 & 0 & 0 & 0 & 4.78 \end{bmatrix}$$

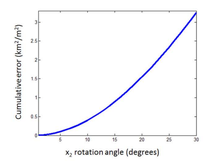

FIG. 6. Cumulative errors for the elastic stiffness parameters as a function of the x_2 rotation angle.

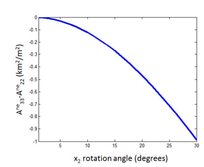

FIG. 7. Plot of A^{ne}_{33} - A^{ne}_{22} as a function of the x_2 rotation angle.

DISSCUSSION AND CONCLUSIONS

- Symmetry axis azimuth is recoverable
- Infer dipping fractures or non-vertical principle stresses
- Knowledge of elastic stiffness parameters provides information regarding fractures and stress fields
- Elasticity provides a common framework for multi-disciplinary studies including seismology, microseismology and geomechanics for an improved characterization of the subsurface